

# Research on the propagation of laser beams array with coherent and incoherent combination in dynamic atmosphere turbulence

WANTAO DENG<sup>1,2\*</sup>, CHENGCHENG WANG<sup>2</sup>, CHUNQUAN GAN<sup>2</sup>, LIANGPING XUE<sup>2</sup>,  
HUIJUN XIA<sup>2</sup>, PENG WANG<sup>2</sup>, HUAN YANG<sup>2</sup>

<sup>1</sup>School of Optics and Photonics, Beijing Institute of Technology, Beijing 100081, China

<sup>2</sup>Southwest Institute of Technical Physics, Chengdu 610041, China

\*Corresponding author: dengwantao@sohu.com

High-power laser systems mostly use coherent or incoherent combined beams to achieve higher laser output power to satisfy the application. However, the far-field beam quality of laser will be reduced when propagating over atmosphere. Based on the propagation model of laser beams array, we use atmospheric coherence length, laser duration and average wind velocity to construct dynamic atmospheric turbulence which is characterized as a phase screen sequence. Meanwhile, considered as the indexes to evaluate beam quality, peak intensity and intensity in bucket are comparatively analysed in coherent and incoherent combined beams in far-field. The results indicate that in weaker turbulence circumstances, coherent combined beam has an advantage compared with the incoherent combined beams when laser duration is short, and coherent combination is more suitable for pulsed laser. With laser duration is increasing, the beam quality of incoherent and coherent combined beams both decrease and tend to be close. In stronger turbulence circumstances, the corresponding laser duration will be shorter when the beam quality of coherent combined beams is extraordinary close to that of incoherent combined beams. The researches can provide important data for high-power laser system to select the optimal beam combination mode to improve its performance.

Keywords: laser propagation, dynamic atmospheric turbulence, coherent combination, incoherent combination, beam quality.

## 1. Introduction

High-power solid laser has extensive application prospects in the field of national defence [1–4]. However, due to the nonlinear effect of the working medium, thermal damage, pump source brightness and other factors, the output power of a single fiber laser with single-mode is limited [5]. In order to obtain an output laser with higher power and better beam quality to satisfy the application of directed energy, it is necessary to build laser array and combine to it to form a single focused beam. At present, the main method of beam combination for high-power laser includes incoherent combi-

nation [6–9], coherent combination [10–13] and spectral combination [14–16]. In fact, no matter which method is chosen, when propagating over atmosphere, the far-field beam quality of laser will inevitably be declined due to atmospheric turbulence. The influence of atmospheric turbulence on laser beams array propagation has been analyzed through simulations and experiments by other researchers [17–21], which sums up the law of different combination after being affected by various atmospheric conditions. In engineering application, an adaptive optics system can correct the wavefront distortion partly caused by atmosphere. Nevertheless, the cost and complexity of high-power laser system will increase accordingly. Therefore, without considering the adaptive optics, scholars pay close attention to the comparison of propagation properties between coherent and incoherent combined beams in atmosphere [22–24]. The common feature of all above studies is that atmospheric turbulence is characterized by analytical function or a static single-phase screen through numerical simulation. However, because the statistical regularities of atmospheric turbulence are related to both space and time, it is of great significance to study the relationship between the time-varying characteristics of atmospheric turbulence and the far-field beam quality. In the present paper, while we propose the propagation model of laser beams array, the time-varying phase screen sequence of atmospheric turbulence is established by such parameters as laser duration  $T$ , average wind velocity  $\bar{v}$  and coherence length  $r_0$ . Then, in order to further explore the comparison of performance for coherent and incoherent beams, we choose the peak intensity  $I_p$  and the intensity in bucket  $I_b$  (the area in bucket of  $I_b$  is defined as the Airy spot area of the ideal plane wave diffracted by a circular aperture which is the same as the whole laser beams array in size). as criteria for measuring the far-field beam quality.

## 2. Principle of constructing phase screen sequence of atmospheric turbulence

The classical approach of constructing a phase screen sequence are frozen turbulence [25] and spline interpolation [26]. Here we will use a spline interpolation method, which is based on adding time variable to static phase screen generated by Zernike polynomials. The static phase screen of atmospheric turbulence can be expressed as [27]

$$\varphi(x, y) = \sum_{k=1}^{\infty} a_k Z_k(x, y) \quad (1)$$

where  $\varphi(x, y)$  becomes dynamic if the  $k$ -th polynomial coefficient  $a_k$  is a time parameter which satisfies specific variation. Therefore, we can suppose that a static phase screen in formula (1) is initial when  $T = 0$ . Then in order to produce a dynamic phase screen sequence, each  $a_k$  changes over time while  $T > 0$ . Such sequence is written as [28]:

$$\varphi(x, y, T) = \sum_{k=1}^{\infty} [1 + X_k(T)] a_k Z_k(x, y) \quad (2)$$

Because the atmospheric turbulence analyzed in this paper is satisfying Kolmogrov spectral distribution, according to Tatarski's model [29], the phase variance of phase screen sequence corresponding to Kolmogrov spectral obeys Gaussian distribution in temporal dimension. Consequently,  $X_k$  in formula (2) represents Gaussian random variables with zero mean and specific variance.

Now if we just pay attention to time-varying state, Eq. (2) can be substituted by

$$\varphi(x, y, T) = \sum_{k=1}^{\infty} b_k(T) Z_k(x, y) \quad (3)$$

where  $b_k(T) = X_k(T)a_k$ . Noll defines the mean square residual error of turbulence phase [30]:

$$\Delta = \int \langle [\Phi(\rho) - \varphi(\rho)]^2 \rangle W(\rho) d(\rho) \quad (4)$$

where  $\rho$  is normalized radial variable in polar coordinates, where the pupil function in a unit circle  $W(\rho)$  has the form:

$$W(\rho) = \begin{cases} 1/\pi, & \rho \leq 1 \\ 0, & \rho > 1 \end{cases} \quad (5)$$

where  $\Phi(\rho)$  denotes the theoretical turbulence phase,  $\varphi(\rho)$ , which is also expressed as Eq. (3), denotes the fitted of turbulence phase; the angled brackets  $\langle \rangle$  indicate the ensemble mean.

Ensemble average is equivalent to time average because the samples used for both satisfy normal distribution which is based on the statistical characteristics of atmospheric turbulence. Hence, if Zernike's polynomials of  $k$  term are used to fit the turbulence phase, Eq. (5) can be simplified as [30]:

$$\Delta_K = \langle \Phi^2 \rangle - \sum_{k=1}^K \langle b_k^2 \rangle \quad (6)$$

Through calculating, Fried had concluded the value of mean square residual  $\Delta_K$  as shown in Table 1 [31].

After substituting the results in Table 1 into Eq. (6), we get the recursive results of  $\langle b_k^2 \rangle$  shown in Table 2.

From Table 2, since  $\langle b_k^2 \rangle$  is determined by optical aperture  $D$  and coherence length  $r_0$ , and  $a_k$  is given, we can calculate the variance of  $X_k(T)$  corresponding to each polynomial in temporal dimension in order to acquire the sequence of  $X_k(T)$  with time-varying. Meanwhile, if this sequence is interpolated, a continuous curve which represents the trend of different Zernike's terms corresponding to the sequence of time-varying phase screen is generated.

Suppose the optical aperture is  $D = 500$  mm and the coherence length is  $r_0 = 10$  cm ( $\lambda = 1080$  nm). After spline interpolation, random nine consecutive images from the

Table 1. Calculation results of  $\Delta_K$ .

$K$	$\Delta_K$
1	$1.0299(D/r_0)^{5/3}$
2	$0.582(D/r_0)^{5/3}$
3	$0.134(D/r_0)^{5/3}$
4	$0.111(D/r_0)^{5/3}$
5	$0.088(D/r_0)^{5/3}$
6	$0.0648(D/r_0)^{5/3}$
7	$0.0587(D/r_0)^{5/3}$
8	$0.0525(D/r_0)^{5/3}$
9	$0.0463(D/r_0)^{5/3}$
10	$0.0401(D/r_0)^{5/3}$
$>10$	$0.2944K^{-\sqrt{3}/2}(D/r_0)^{5/3}$

Table 2. Calculations results of  $\langle b_k^2 \rangle$ .

$k$	$\langle b_k^2 \rangle$
2	$\Delta_1 - \Delta_2 = 0.448(D/r_0)^{5/3}$
3	$\Delta_2 - \Delta_3 = 0.448(D/r_0)^{5/3}$
4	$\Delta_3 - \Delta_4 = 0.023(D/r_0)^{5/3}$
5	$\Delta_4 - \Delta_5 = 0.023(D/r_0)^{5/3}$
6	$\Delta_5 - \Delta_6 = 0.023(D/r_0)^{5/3}$
7	$\Delta_6 - \Delta_7 = 0.0062(D/r_0)^{5/3}$
8	$\Delta_7 - \Delta_8 = 0.0062(D/r_0)^{5/3}$
9	$\Delta_8 - \Delta_9 = 0.0062(D/r_0)^{5/3}$
10	$\Delta_9 - \Delta_{10} = 0.0062(D/r_0)^{5/3}$
...	...
$K$	$\Delta_{K-1} - \Delta_K = -0.2944[K^{-\sqrt{3}/2} - (K-1)^{-\sqrt{3}/2}](D/r_0)^{5/3}$

phase screen sequence are shown in Fig. 1. Here we find that the variation of the phase screen generated by the interpolation method is smooth, which could simulate the atmospheric turbulence in real circumstances.

### 3. Relationship between phase screen sequence and laser duration

For the high-power laser system with energy-applied, we mainly focus on the energy concentration degree of the accumulated spot formed by laser propagating to the target in a certain duration, so the relationship between the phase screen sequence and laser duration is analysed in this section. Fried defined the coherence length  $r_0$  [31] and the coherence time  $\tau_0$  [32] from spatial and temporal dimension, respectively. As another

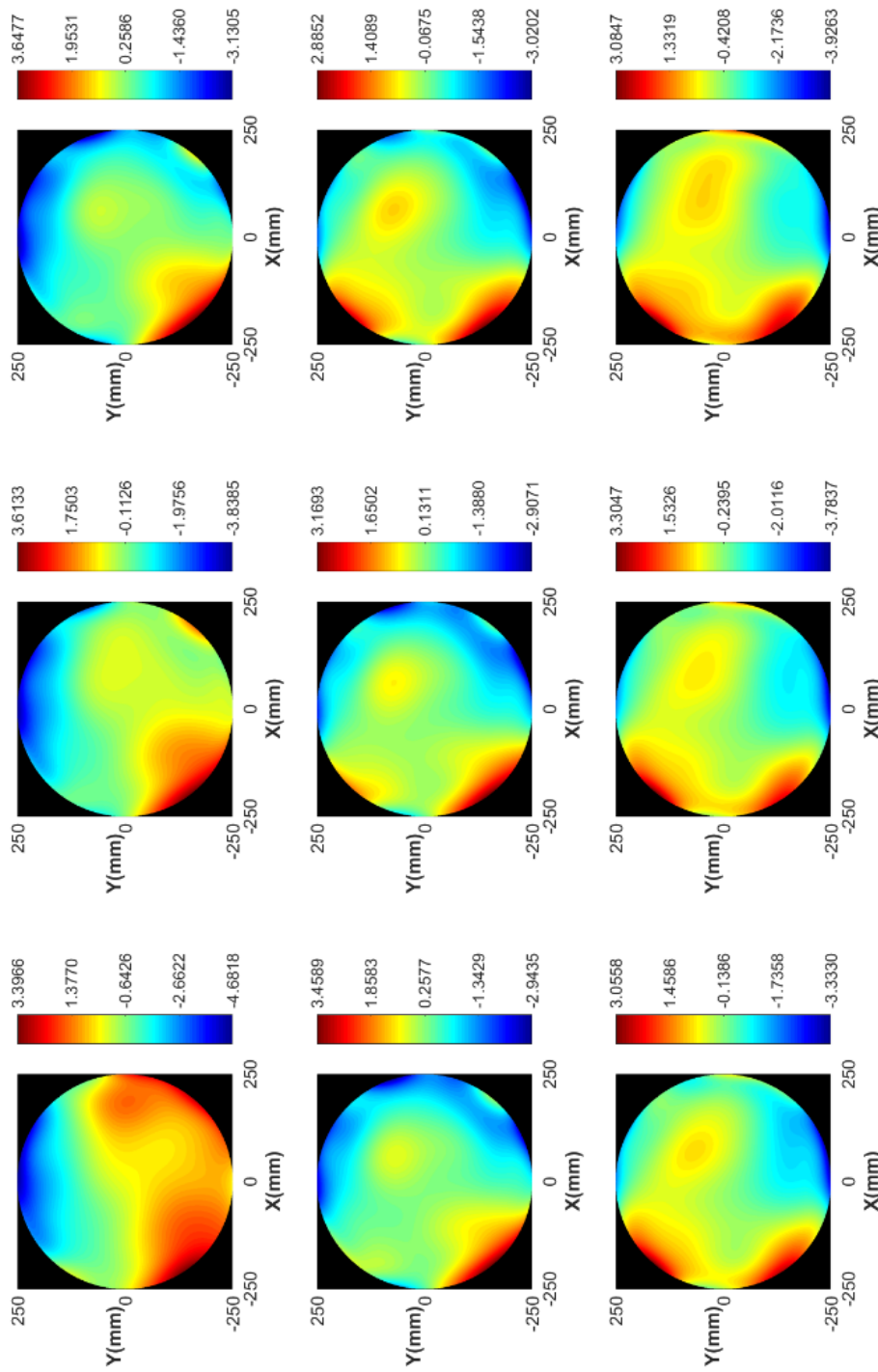


Fig. 1. Atmospheric turbulence phase screen changing continuously (from left to right, from top to bottom).

important atmospheric parameter,  $\tau_0$  represents the time correlation of the wavefront affected by the atmosphere, which can be explained that if the time interval between two different wavefronts arriving at observation exceeds  $\tau_0$ , the phases between them are no longer correlated. After calculation, the relevance of  $r_0$  and  $\tau_0$  is described by the following formula [33]:

$$\tau_0 = 0.314 \frac{r_0}{\bar{v}} \quad (7)$$

where  $\bar{v}$  is the tangential average wind velocity on the path of propagation.

According to the hypothesis of atmospheric turbulence freezing [34, 35], the spatial distribution of turbulent wavefront does not change in short time. However, it will translationally move affected by tangential wind. Suppose  $t$  is the time of the turbulent wavefront completely passing through the optical aperture of diameter  $D$  when the tangential average wind velocity is  $\bar{v}$ . Therefore, after  $t$ , the turbulent wavefront in  $D$  can be represented by another random wavefront which also fits the statistical rule of Kolmogorov spectrum.  $t$  can be expressed as:

$$t = D/\bar{v} \quad (8)$$

From Eq. (8), if laser duration is  $T$ , the corresponding number  $N_u$  of the phase screen sequence is written as:

$$N_u = \frac{T}{t} = T \frac{\bar{v}}{D} \quad (9)$$

According to the definition of  $\tau_0$ , the atmospheric turbulence which originally conforms to the statistical rule of Kolmogorov spectrum no longer conforms to such rule after  $\tau_0$ . Consequently, in order to maintain the statistical rule of Kolmogorov spectrum of each atmospheric turbulence phase screen, it is necessary to interpolate every interval of  $\tau_0$ .

Combined with Eq. (8) and Eq. (9), the number of frames  $N_i$  to be interpolated between two phase screens can be expressed as:

$$N_i \geq \frac{t}{\tau_0} = 3.18 \frac{D}{r_0} \quad (10)$$

The total number of frames of phase screen sequence  $N_t$  is given by:

$$N_t = N_u + N_i(N_u - 1) \quad (11)$$

When continuous laser with different duration propagates through atmosphere, the phase screen sequence of  $N_t$  frame can characterize atmospheric turbulence. If laser duration is shorter, it can be equivalent to the pulse width of pulse laser. The hypothesis

of atmospheric turbulence freezing [35] tell us that atmospheric turbulence can be assumed to be “frozen” from milliseconds to tens of milliseconds. So, for a single pulse laser with pulse width  $\tau$ , if we set the appropriate number of interpolations so that  $N_t \leq 1/\tau$  when  $T = 1$  s, just a single-phase screen can characterize atmospheric turbulence.

#### 4. Distribution of laser beams array in near-field

The model of laser beams array modulated by optical emitting antenna propagating to the receiver plane is shown in Fig. 2.

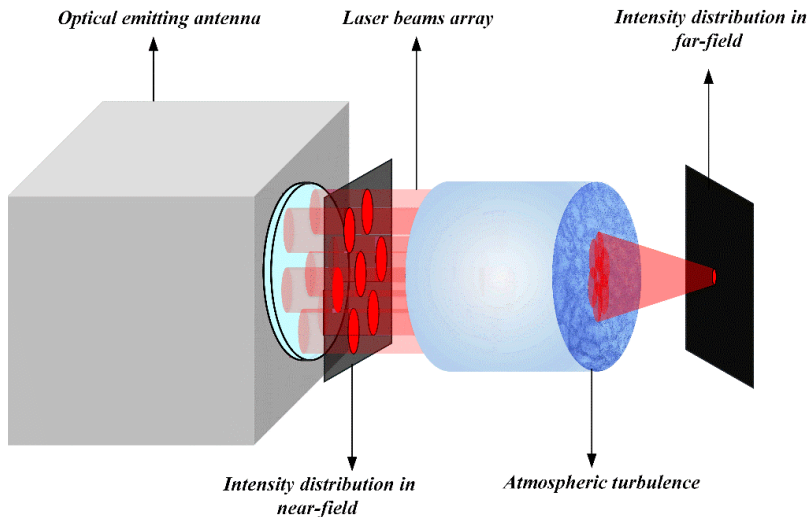


Fig. 2. Model of propagation of laser beams array.

Assume that the complex amplitude of the sub beam obeys the Gaussian distribution of fundamental mode normalized, and all the beams distribute in radial. The whole complex amplitude distribution at the exit of an optical emitting antenna is written as:

$$\begin{aligned} U_{0j}(x, y) &= \\ &= \exp \left\{ \frac{1}{\omega_0^2} \left[ \left( x - \left| \sin \left( j \frac{\pi}{2} \right) \right| r \cos(j\theta) \right)^2 + \left( y - \left| \sin \left( j \frac{\pi}{2} \right) \right| r \sin(j\theta) \right)^2 \right] + i\psi_j \right\} \end{aligned} \quad (12)$$

where  $j$  denotes the number of sub beams,  $r$  denotes the radial distance between the central beam and the others,  $\theta = 360^\circ/(N-1)$  is the angle between the adjacent fringe beam,  $\omega_0$  is the waist of each sub beam,  $\psi_j$  is the phase of the  $j$ -th sub-beam.

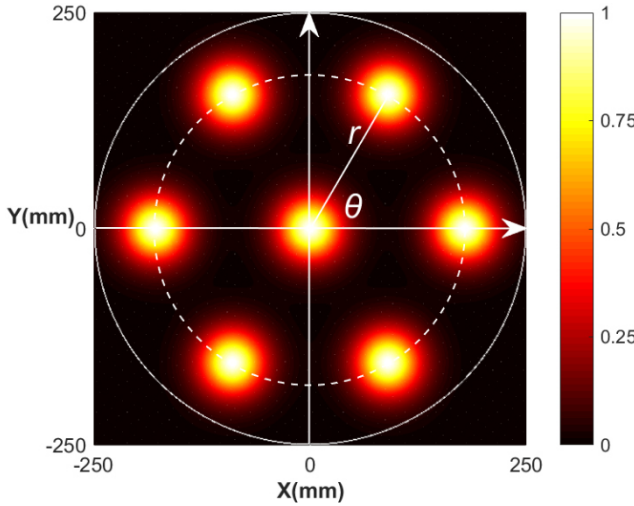


Fig. 3. Intensity distribution in the near-field.

Suppose  $N = 7$ , then  $\theta = 60^\circ$ . If the diameter of the whole laser beams array is  $D = 500$  mm and the divergence of the sub beam is  $\Theta = 20 \mu\text{rad}$ , the intensity distribution in the near-field is shown in Fig. 3.

## 5. Propagation of combined beams

In far-field, when propagating convergently, the intensity distribution of incoherently combined beams should be the sum of the intensity distribution of the sub beam. While the distance of propagation is  $L$  (from  $z_0$  to  $z_L$ ), the complex amplitude of each sub beam is modulated by a spherical wave with curvature radius  $2L$ , and it is expressed as:

$$U_{1j}(x, y, z_L) = U_{0j}(x, y, z_L) \exp\left(-\frac{2\pi}{\lambda} \frac{x^2 + y^2}{2L}\right) \quad (13)$$

According to the theory of angular spectrum [36], the complex amplitude of the  $j$ -th sub-beam propagating  $L$  in dynamic atmospheric turbulence can be expressed as:

$$\begin{aligned} U_{2j}(x, y, z_L) &= \\ &= F^{-1} \left\{ F \left[ U_{1j}(x, y, z_L) \exp(i\varphi(x, y, T)) \right] \exp \left[ -i \frac{2\pi}{\lambda} L \sqrt{1 - (\lambda f_x)^2 - (\lambda f_y)^2} \right] \right\} \end{aligned} \quad (14)$$

where  $F$  and  $F^{-1}$  are Fourier transform and inverse Fourier transform, respectively,  $f_x$  and  $f_y$  are spatial frequencies in  $x$  and  $y$  directions, respectively. The intensity of incoherently combined beams in far-field is written as:

$$U_{\text{incoherent}}(x, y, z_L) = \sum_{j=0}^{N-1} \left[ U_{2j}(x, y, z_L) U_{2j}^*(x, y, z_L) \right] \quad (15)$$

For coherently combined beams, the phase  $\psi_j$  of each sub beam is consistent, and the intensity in far-field is obtained by the product of the complex amplitude of beams array and its conjugate. When propagating  $L$  in dynamic atmospheric turbulence, the intensity of coherently combined beams in far-field is deduced as follows:

$$U_1(x, y, z_0) = \left[ \sum_{j=0}^{N-1} U_{0j}(x, y, z_L) \right] \exp\left(-\frac{2\pi}{\lambda} \frac{x^2 + y^2}{2L}\right) \quad (16)$$

$$\begin{aligned} U_2(x, y, z_L) &= \\ &= F^{-1} \left\{ F \left[ U_1(x, y, z_0) \exp(i\varphi(x, y, T)) \right] \exp \left[ -i \frac{2\pi}{\lambda} L \sqrt{1 - (\lambda f_x)^2 - (\lambda f_y)^2} \right] \right\} \end{aligned} \quad (17)$$

$$U_{\text{coherent}}(x, y, z_L) = U_2(x, y, z_L) U_2^*(x, y, z_L) \quad (18)$$

According to the parameter in Table 3, for comparison, we suppose that in free-space, the total energy of continuous laser in duration is the same as that of pulse laser, and the atmospheric turbulence phase screen or sequence used to modulate wave front for such two laser systems mentioned above is identical.

Table 3. Simulation parameters.

Type	Value
Coherence length $r_0$ at $\lambda = 1080$ nm	10 cm
Average wind velocity $\bar{v}$	2 m/s
Propagation distance $L$	5 km
Number of combined beams $N$	7
Continuous laser duration $T$	3s
Pulsed laser duration $\tau$	1 ms
Pulsed laser frequency $f$	1 Hz

As shown in Figs. 4a and 4b, the  $I_p$  of coherent combined beam is 7 times higher than that of incoherent combined beam in free-space. Then, Figs. 4c and 4d tell us that when laser duration is shorter ( $\tau = 1$  ms) in atmosphere, the  $I_p$  of coherent combined beam is less 4 times of that of incoherent combined beam. Finally, it can be seen from Figs. 4e and 4f that when laser duration is longer ( $T = 3$  s) in atmosphere, the  $I_p$  of coherent combined beam is almost the same as that of incoherent combined beam.

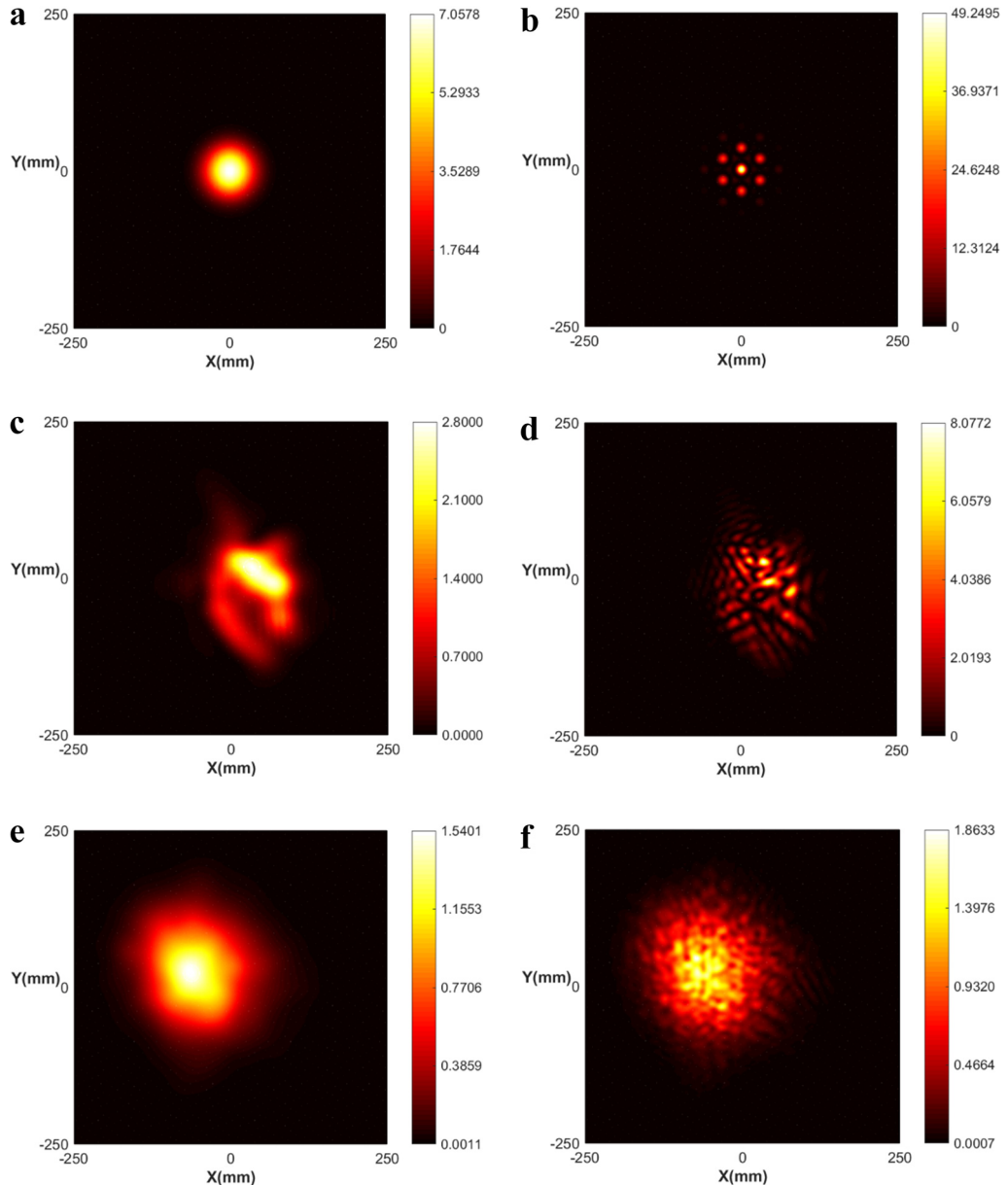


Fig. 4. Intensity distributions in far-field: (a) incoherently combined beams, pulsed or continuous, propagation in free-space; (b) coherently combined beams, continuous or pulsed, propagation in free-space; (c) incoherently combined beams, pulsed, propagation in turbulent atmosphere; (d) coherently combined beams, pulsed, propagation in turbulent atmosphere; (e) incoherently combined beams, continuous, propagation in turbulent atmosphere; (f) coherently combined beams, continuous, propagation in turbulent atmosphere.

## 6. Numerical results

In order to further explore the influence of the propagation performance of coherently combined beams and incoherently combined beams by atmospheric turbulence, we set coherence length and laser duration as variables and keep other parameters constant in Table 3. We consider the pulse laser duration as  $T=0$  s to make comparative analyzes in a chart convenient. As shown in Figs. 5 and 6, after calculating, we get the relationship between  $I_p$ ,  $I_b$  and laser duration  $T$  when coherence length  $r_0 = 10$  cm, 20 cm, and 40 cm.

Figures 5a and 6a show that the far-field beam quality of laser beams array in free-space is constant, and coherent combination has great advantage compared with incoherent combination. We take  $\Delta I_p = I_{p(\text{coherent})} - I_{p(\text{incoherent})}$  and  $\Delta I_b = I_{b(\text{coherent})} - I_{b(\text{incoherent})}$  in free-space as standards to normalize in atmosphere with different  $r_0$  and  $T$ . The larger

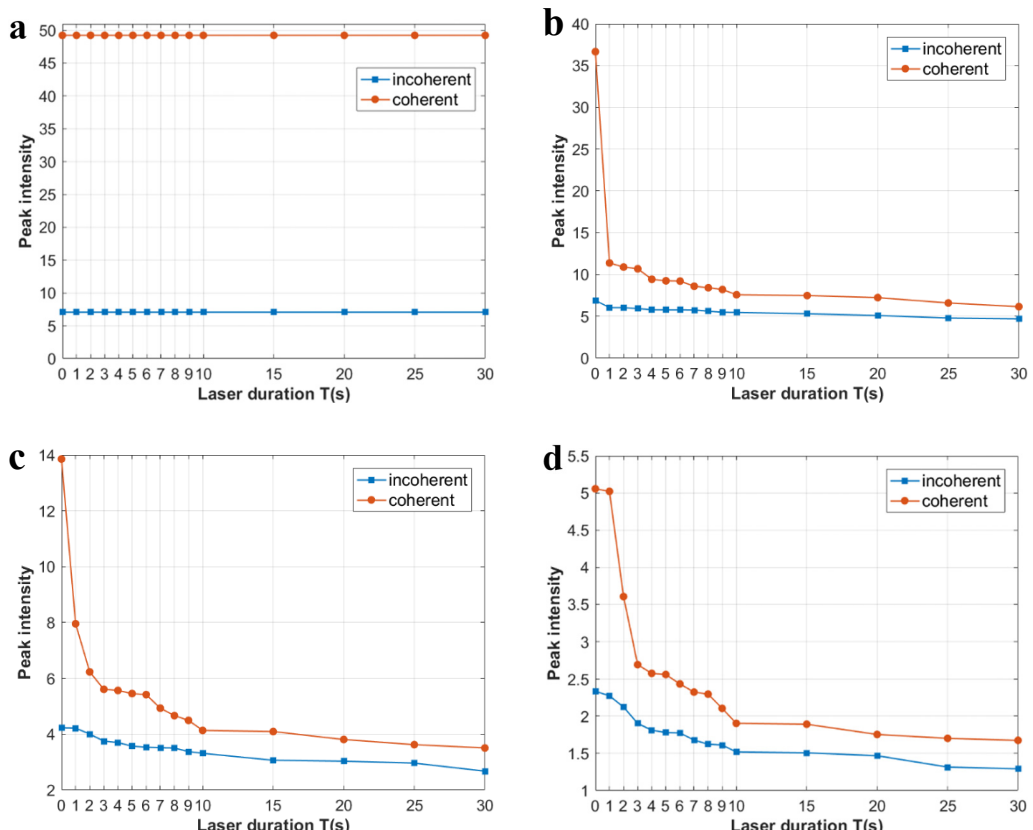


Fig. 5. Peak Intensity  $I_p$  under conditions of laser duration: (a) propagation in free-space; (b) propagation in turbulent atmosphere,  $r_0 = 40$  cm; (c) propagation in turbulent atmosphere,  $r_0 = 20$  cm; (d) propagation in turbulent atmosphere,  $r_0 = 10$  cm.

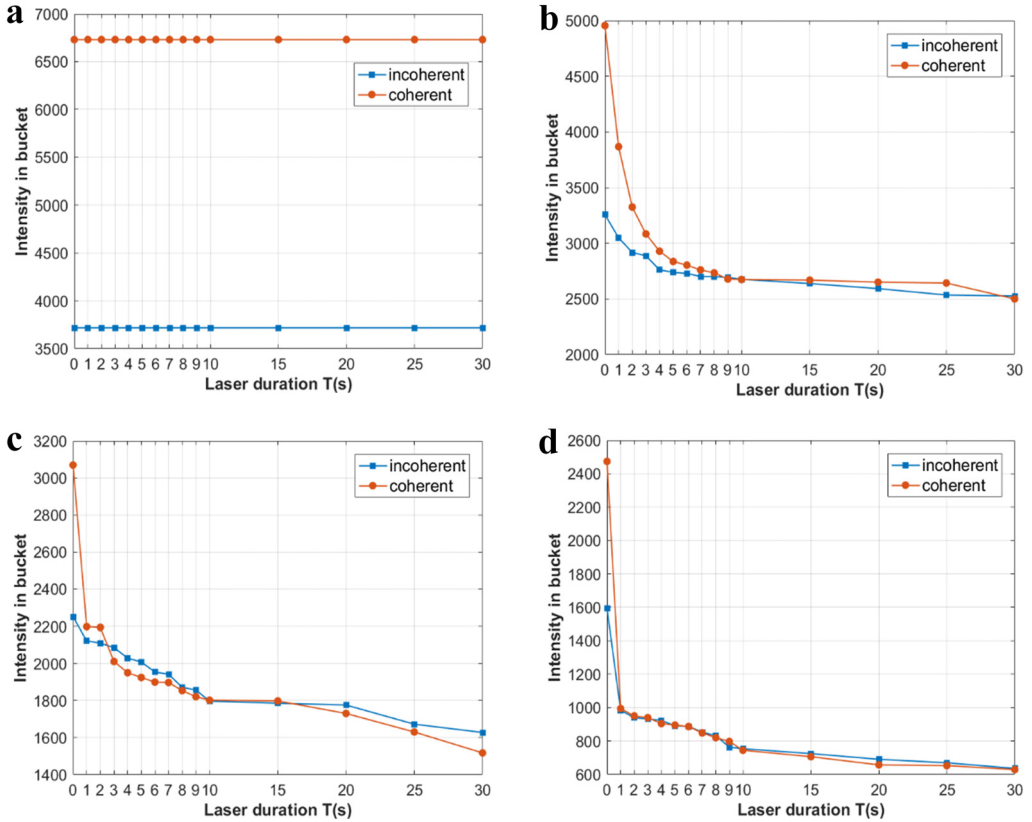


Fig. 6. Intensity in bucket  $I_b$  under conditions of laser duration: (a) propagation in free-space; (b) propagation in turbulent atmosphere,  $r_0 = 40$  cm; (c) propagation in turbulent atmosphere,  $r_0 = 20$  cm; (d) propagation in turbulent atmosphere,  $r_0 = 10$  cm.

Table 4. Statistical results of  $\Delta I_p$  and  $\Delta I_b$ .

Coherence length $r_0$ [cm]	Normalized $\Delta I_p$				Normalized $\Delta I_b$			
	$T = 0$ s	$T = 5$ s	$T = 10$ s	$T = 30$ s	$T = 0$ s	$T = 5$ s	$T = 10$ s	$T = 30$ s
40	70.5%	8.5%	5%	3.5%	56.3%	3.2%	0.1%	0.8%
20	22.8%	7.4%	1.9%	1.9%	29.2%	2.7%	-0.1%	-0.2%
10	6.4%	1.8%	0.9%	0.9%	27.1%	0.1%	-0.3%	-3.6%

the normalized value, the more obvious the advantage of coherent combination. But if the normalized value is negative, the incoherent combination is better. The statistical results are shown in Table 4.

Figures 5b–5d and 6b–6d can illustrate that the far-field beam quality is better and the superiority of coherent combination is more evident if  $T$  is shorter, especially when the pulse laser is chosen, but with the increase of  $T$ , the far-field beam quality becomes worse and coherent combination is no longer available. It is also confirmed in Table 4,

suppose  $r_0 = 40\text{cm}$ , when  $T$  increases from 0 to 30 s, normalized  $\Delta I_p$  decreased from 70.5% to 3.5% and normalized  $\Delta I_b$  decreased from 56.3% to -0.8%. In addition, if  $r_0$  decreases, the far-field beam quality gets worse and the superiority of coherent combination weakens faster. For example, in Table 4, if  $r_0 = 40\text{ cm}$  and  $T = 30\text{ s}$ , normalized  $\Delta I_p$  is 3.5% and normalized  $\Delta I_b$  is 0.8%. Nevertheless, normalized  $\Delta I_p$  becomes only 1.8% and normalized  $\Delta I_b$  becomes only 0.1% when  $r_0 = 10\text{ cm}$  and  $T = 5\text{ s}$ .

## 7. Discussions and conclusions

In this paper, we analyze the effect of dynamic atmospheric turbulence on laser beams array propagating based on the model of coherent combination and incoherent combination, respectively. The results demonstrate following conclusions:

- 1) Coherent combination possesses attractive advantages, *i.e.* the constructive interference caused by the same central phase of each sub beam, which makes the intensity distribution in far-field appear characteristic with extremely high peak intensity of the main lobe.
- 2) The beam quality of coherent combination is better than that of incoherent combination under the condition of shorter laser duration and shorter coherence length, and coherent combination is more suitable for pulsed laser. When laser duration increases, the beam quality of the two decreases to stable condition and tend to be consistent. There are two reasons for this phenomenon. The one is that the turbulent wavefront causes the spot expanding and the peak intensity descending in far-field, and the other one is that the position of the peak intensity alters randomly due to the turbulent wavefront changing over time, which makes it characteristic that with extremely high peak intensity the main lobe is no longer significant.
- 3) It takes less time for the beam quality of coherent combination to reduce to steady state if coherence length is longer, because the turbulent wavefront distorted more seriously can cause the destruction of coherence faster, which results in the intensity distribution of coherent combination evolving to be unanimous with that of incoherent combination. To sum up, in the application of the high-power laser system, in order to achieve a higher cost-effectiveness ratio, how to design the roadmap is related to system requirements, technical complexity and economy principles. The results of our research presented in this paper just show the key support for selecting a combination mode.

## References

- [1] SPRANGLE P., HAFIZI B., TING A., FISCHER R.P., DAVIS C.C., NELSON W., *High-power lasers for directed-energy applications: reply*, Applied Optics **56**(16), 2017, pp. 4825–4826, DOI: [10.1364/AO.56.004825](https://doi.org/10.1364/AO.56.004825).
- [2] VORONTSOV M.A., WEYRAUCH T., *High-power lasers for directed-energy applications: comment*, Applied Optics **55**(35), 2016, pp. 9950–9953, DOI: [10.1364/AO.55.009950](https://doi.org/10.1364/AO.55.009950).
- [3] PANDEY R., MERCHEN D., STAPLETON D., PATTERSON S.G., *Advancements in high-power diode laser stacks for defense applications*, Proc. SPIE **8381**, Laser Technology for Defense and Security VIII, 83810G (7 May 2012), DOI: [10.1117/12.916743](https://doi.org/10.1117/12.916743).

- [4] O'CONNER M., *High power fiber lasers for defense applications*, [in] *Lasers, Sources, and Related Photonic Devices*, OSA Technical Digest (CD), San Diego, 2012, paper FW3C.1, DOI: [10.1364/FILAS.2012.FW3C.1](https://doi.org/10.1364/FILAS.2012.FW3C.1).
- [5] ZERVAS M.N., CODEMAR C.A., *High power fiber lasers: a review*, IEEE Journal of Selected Topics in Quantum Electronics **20**(5), 2014, pp. 219–241, DOI: [10.1109/JSTQE.2014.2321279](https://doi.org/10.1109/JSTQE.2014.2321279).
- [6] WU C., ZHANG R., *Study on the superposition characteristics of distorted beam in far field*, Optik **127**(4), 2016, pp. 1748–1753, DOI: [10.1016/j.ijleo.2015.11.003](https://doi.org/10.1016/j.ijleo.2015.11.003).
- [7] TAO R.M., SI L., MA Y.X., ZOU Y.C., ZHOU P., *Tolerance on tilt error for the incoherent combination of fiber lasers in a real environment*, Chinese Physics Letters **28**(7), 2011, article 074219, DOI: [10.1088/0256-307X/28/7/074219](https://doi.org/10.1088/0256-307X/28/7/074219).
- [8] ZHOU X.Y., CHEN Z.L., WANG Z.F., HOU J., XU X.J., *High-power incoherent beam combining of fiber lasers based on a 7 × 1 all-fiber signal combiner*, Optical Engineering **55**(5), 2016, article 056103, DOI: [10.1117/1.OE.55.5.056103](https://doi.org/10.1117/1.OE.55.5.056103).
- [9] LEI C., GU Y., CHEN Z., WANG Z., ZHOU P., MA Y., XIAO H., LENG J., WANG X., HOU J., XU X., CHEN J., LIU Z., *Incoherent beam combining of fiber lasers by an all-fiber 7 × 1 signal combiner at a power level of 14 kW*, Optics Express **26**(8), 2018, pp. 10421–10427, DOI: [10.1364/oe.26.010421](https://doi.org/10.1364/oe.26.010421).
- [10] WANG X.L., MA Y.X., ZHOU P., HE B., XIAO H., XUE Y.H., LIU C., LI Z., XU X.J., ZHOU J., LIU Z., ZHAO Y., *Coherent beam combining of 137 W 2 × 2 fiber amplifier array*, Optics Communications **284**(8), 2011, pp. 2198–2201, DOI: [10.1016/j.optcom.2010.12.090](https://doi.org/10.1016/j.optcom.2010.12.090).
- [11] KASHANI F.D., ALAVINEJAD M., GHAFARY B., *Coherence characterization of partially coherent flat-topped beam propagating through atmospheric turbulence*, Optica Applicata **39**(2), 2009, pp. 429–440.
- [12] ZHOU P., WANG X.L., MA Y.X., MA H.T., XU X.J., LIU Z.J., *Propagation of partially coherent partially phase-locked laser array in turbulent atmosphere*, Optics Communications **283**(6), 2010, pp. 1071–1074, DOI: [10.1016/j.optcom.2009.10.118](https://doi.org/10.1016/j.optcom.2009.10.118).
- [13] WEYRAUCH T., VORONTSOV M., MANGANO J., OVCHINNIKOV V., BRICKER D., POLNAU E., ROSTOV A., *Deep turbulence effects mitigation with coherent combining of 21 laser beams over 7 km*, Optics Letters **41**(4), 2016, pp. 840–843, DOI: [10.1364/OL.41.000840](https://doi.org/10.1364/OL.41.000840).
- [14] RANA P., MISHRA S.K., SAHOO S.P., BHALE D., SRIDHAR G., RAWAT V.S., *Co-amplification: an efficient spectral beam combination approach for high power, closely separated dual wavelength dye laser systems*, Optics Communications **451**, 2019, pp. 367–373, DOI: [10.1016/j.optcom.2019.06.064](https://doi.org/10.1016/j.optcom.2019.06.064).
- [15] TIAN J.Y., ZHANG J., PENG H.Y., LEI Y.X., QIN L., NING Y.Q., WANG L.J., *High power diode laser source with a transmission grating for two spectral beam combining*, Optik **192**, 2019, article 162918, DOI: [10.1016/j.ijleo.2019.06.018](https://doi.org/10.1016/j.ijleo.2019.06.018).
- [16] SUN F.Y., ZHAO Y.F., SU S.L., HOU G.Y., LU Z.Y., ZHANG X., WANG L.J., TIAN S.C., TONG C.Z., WANG L.J., *High beam quality broad-area diode lasers by spectral beam combining with double filters*, Chinese Optics Letters **17**(01), 2019, article 011401, DOI: [10.3788/COL201917.011401](https://doi.org/10.3788/COL201917.011401).
- [17] NELSON W., SPRANGLE P., DAVIS C.C., *Atmospheric propagation and combining of high-power lasers: reply*, Applied Optics **55**(29), 2016, pp. 8338–8339, DOI: [10.1364/AO.55.008338](https://doi.org/10.1364/AO.55.008338).
- [18] MAHDIEH M.H., *Numerical approach to laser beam propagation through turbulent atmosphere and evaluation of beam quality factor*, Optics Communications **281**(13), 2008, pp. 3395–3402, DOI: [10.1016/j.optcom.2008.02.040](https://doi.org/10.1016/j.optcom.2008.02.040).
- [19] LAZER N., ARUL TEEN Y.P., *Free Space Optical Communication and Laser Beam Propagation through Turbulent Atmosphere: A Brief Survey*, 2019 International Conference on Recent Advances in Energy-efficient Computing and Communication (ICRAECC), Nagercoil, India, 2019, pp. 1–6, DOI: [10.1109/ICRAECC43874.2019.8994973](https://doi.org/10.1109/ICRAECC43874.2019.8994973).
- [20] GOLMOHAMMADY S., GHAFARY B., *The polarization and coherence behavior of the flat-topped array beam through non-Kolmogorov turbulence*, Optica Applicata **49**(1), 2019, pp. 75–88, DOI: [10.5277/oa190107](https://doi.org/10.5277/oa190107).
- [21] KULIKOV V.A., VORONTSOV M.A., *Analysis of the joint impact of atmospheric turbulence and refractivity on laser beam propagation*, Optics Express **25**(23), 2017, pp. 28524–28535, DOI: [10.1364/oe.25.028524](https://doi.org/10.1364/oe.25.028524).

- [22] TADAYYONI S., SHAYGANMANESH M., *Investigation of coherent and incoherent laser beams propagation through turbulent atmosphere*, International Journal Optics and Photonics **13**(2), 2019, pp. 145–154, DOI: [10.29252/ijop.13.2.145](https://doi.org/10.29252/ijop.13.2.145).
- [23] ZHOU P., LIU Z.J., XU X.J., CHU X.X., *Comparative study on the propagation performance of coherently combined and incoherently combined beams*, Optics Communications **282**(8), 2009, pp. 1640–1647, DOI: [10.1016/j.optcom.2009.01.011](https://doi.org/10.1016/j.optcom.2009.01.011).
- [24] GRASSO R.J., *Atmospheric propagation of coherently and incoherently combined quantum cascade lasers*, Proc. SPIE **10408**, Laser Communication and Propagation through the Atmosphere and Oceans VI, 104080A (31 August 2017), DOI: [10.1117/12.2275867](https://doi.org/10.1117/12.2275867).
- [25] ANDREWS L.C., PHILLIPS R.L., *Laser Beam Propagation through Random Media*, SPIE Press, 2005, DOI: [10.1117/3.626196](https://doi.org/10.1117/3.626196).
- [26] PHILLIPS J.D., GODA M.E., SCHMIDT J., *Atmospheric turbulence simulation using liquid crystal spatial light modulators*, Proc. SPIE **5894**, Advanced Wavefront Control: Methods, Devices, and Applications III, 589406 (22 August 2005), DOI: [10.1117/12.620407](https://doi.org/10.1117/12.620407).
- [27] RODDIER N.A., *Atmospheric wavefront simulation using Zernike polynomials*, Optical Engineering, **29**(10), 1990, pp. 1174–1180, DOI: [10.1117/12.55712](https://doi.org/10.1117/12.55712).
- [28] WILCOX C.C., SANTIAGO F., MARTINEZ T., ANDTEWS J.R., RESTAINO S.R., CORLEY M., TEARE S.W., AGRAWAL B.N., *A method of generating atmospheric turbulence with a liquid crystal spatial light modulator*, Proc. SPIE **7816**, Advanced Wavefront Control: Methods, Devices, and Applications VIII, 78160E (12 August 2010), DOI: [10.1117/12.861510](https://doi.org/10.1117/12.861510).
- [29] TATARSKI V.I., *Wave Propagation in a Turbulent Medium*, McGraw, 1961.
- [30] NOLL R.J., *Zernike polynomials and atmospheric turbulence*, Journal of the Optical Society of America **66**(3), 1976, pp. 207–211, DOI: [10.1364/JOSA.66.000207](https://doi.org/10.1364/JOSA.66.000207).
- [31] FRIED D.L., *Statistics of a geometric representation of wavefront distortion*, Journal of the Optical Society of America **55**(11), 1965, pp. 1427–1435, DOI: [10.1364/JOSA.55.001427](https://doi.org/10.1364/JOSA.55.001427).
- [32] FRIED D.L., *Time-delay-induced mean-square error in adaptive optics*, Journal of the Optical Society of America A **7**(7), 1990, pp. 1224–1225, DOI: [10.1364/JOSAA.7.001224](https://doi.org/10.1364/JOSAA.7.001224).
- [33] THOMPSON L., *Adaptive Optics in Astronomy (Edited by François Roddier)*, Physics Today **53**(4), 2000, p. 69, DOI: [10.1063/1.2405462](https://doi.org/10.1063/1.2405462).
- [34] SCHOCK M., SPILLAR E.J., *Method for a quantitative investigation of the frozen flow hypothesis*, Journal of the Optical Society of America A **17**(9), 2000, pp. 1650–1658, DOI: [10.1364/JOSAA.17.001650](https://doi.org/10.1364/JOSAA.17.001650).
- [35] POYNEER L., VAN DAM M., VÉRAN J.P., *Experimental verification of the frozen flow atmospheric turbulence assumption with use of astronomical adaptive optics telemetry*, Journal of the Optical Society of America A **26**(4), 2009, pp. 833–846, DOI: [10.1364/josaa.26.000833](https://doi.org/10.1364/josaa.26.000833).
- [36] VOELZ D.G., *Computational Fourier Optics: A MATLAB Tutorial*, SPIE Press, 2011.

Received March 5, 2021  
in revised form May 1, 2021